

AN AERODYNAMIC ANALYSIS OF BIRD WINGS AS FIXED AEROFOILS

By PHILIP C. WITHERS

*Department of Biology, Portland State University, P.O. Box 751,
Portland, Oregon 97207*

(Received 5 March 1980)

SUMMARY

The aerodynamic properties of bird wings were examined at Reynolds numbers of $1-5 \times 10^4$ and were correlated with morphological parameters such as aspect ratio, camber, nose radius and position of maximum thickness. The many qualitative differences between the aerodynamic properties of bird, insect and aeroplane wings are attributable mainly to their differing Reynolds numbers. Bird wings, which operate at lower Reynolds numbers than aerofoils, have high minimum drag coefficients (0.03-0.13), low maximum lift coefficients (0.8-1.2) and low maximum lift/drag ratios (3-17). Bird and insect wings have low aerofoil efficiency factors (0.2-0.8) compared to conventional aerofoils (0.9-0.95) because of their low Reynolds numbers and high profile drag, rather than because of a reduced mechanical efficiency of animal wings.

For bird wings there is clearly a trade-off between lift and drag performance. Bird wings with low drag generally had low maximum lift coefficients whereas wings with high maximum lift coefficients had high drag coefficients. The pattern of air flow over bird wings, as indicated by pressure-distribution data, is consistent with aerodynamic theory for aeroplane wings at low Reynolds numbers, and with the observed lift and drag coefficients.

INTRODUCTION

The theory of animal flight can be better understood than the theory of many other aspects of animal energetics and locomotion, by making use of classical fluid dynamic and modern aerofoil theory. The fluid-dynamic basis for lift and drag applies equally to man-made and animal aerofoils, and our present understanding of bird flight is mostly derived from aerofoil theory with only some recourse to empirical data for birds (e.g. Pennycuik, 1969, 1975; Tucker, 1968, 1972, 1973; Weis-Fogh, 1973, 1976; Greenewalt, 1975; Rayner, 1979). However, aerofoil data cannot be extrapolated directly to avian and insect flight, but must be scaled according to the Reynolds number (Re). Bird wings generally operate at Re 's below a critical transition range (10^4-10^6), where lift and drag coefficients alter markedly (Von Mises, 1959; Hoerner, 1965; Hoerner & Borst, 1975). Empirical studies of bird wings (Nachtigall & Kempf, 1971; Reddig, 1978; Nachtigall, 1979) and insect wings dramatically illustrate the aerodynamic consequences of a low Re (see also Nachtigall, 1977; Jensen, 1956; Vogel, 1966).

The primary objectives of the present study are to investigate the basic aerodynamic properties of isolated, fixed bird wings at their appropriate Re , to determine how the aerodynamic properties are affected by wing morphology, and to compare their performance with that of conventional aerofoils (working at high Re) and insect wings (low Re). The basic aerodynamic measurements are: lift and drag coefficients at varying angles of attack, minimum drag coefficient, maximum lift coefficient, maximum lift/drag ratio, and aerofoil efficiency factor. The role of wing-tip slots, a complication due to bird wings being composed of many laminated feathers, is considered elsewhere (P. C. Withers, in preparation) but basic aerodynamic data for a single primary feather from a black vulture are presented here as a comparison for the data concerning complete wings.

METHODS

Bird wings. Bird wings, dried in an appropriate gliding position, were used. Wings were obtained from frozen birds or were borrowed from the ornithology collection of the Duke University Zoology Department. A brass rod was glued inside the humerus with epoxy resin, and the rod was mounted directly on a force transducer assembly. Separation of the primary feathers did not occur for any species at positive angles of attack. Only the hawk wing had wing-tip slots.

Wings from the following species were studied: European starling (*Sturnidae*; *Sturnus vulgaris*); common nighthawk (*Caprimulgidae*; *Chordeiles minor*); chimney swift (*Apodidae*; *Chaetura pelagica*); Leach's petrel (*Hydrobatidae*; *Oceanodroma leucorhoa*); bobwhite quail (*Phasianidae*; *Colinus virginianus*); wood duck (*Anatidae*; *Aix sponsa*); American woodcock (*Scolopidae*; *Philohela minor*); red-shouldered hawk (*Accipitridae*; *Buteo lineatus*). The tip of a primary feather from a black vulture (*Coragyps atratus*) was also studied. Body mass and wing loading of these species are: starling, 0.0850 kg, 4.3 kg m⁻²; nighthawk, 0.064 kg, 1.9 kg m⁻²; chimney swift, 0.017 kg, 1.7 kg m⁻²; petrel, 0.027 kg, 1.1 kg m⁻²; quail, 0.150 kg, 9.2 kg m⁻²; wood duck, 0.590 kg m⁻²; woodcock, 0.200 kg, 5.6 kg m⁻²; hawk, 0.550 kg, 3.3 kg m⁻² (Poole, 1938; Hartman, 1961).

The length of the wing, from tip to point of attachment at the humerus (i.e. wing semi-span), was measured to the nearest millimetre and the projected wing area was calculated by weighing tracings of the wing outline. Average wing cord (\bar{c}) and aspect ratio (AR) were then calculated as:

$$\bar{c} = \text{wing area} / \text{wing semi-span}, \quad AR = \text{wing area} / (\text{wing semi-span})^2.$$

Chord-wise cross-sections of the large wings were determined by cutting and fitting paper templates to the upper and lower wing surfaces; for the small wings and vulture feather a three-dimensional micromanipulator was employed. These local cross-sections were used to calculate the average value for the wing of section chord to section perimeter. The surface area of the wing ('wetted area') was then calculated from the projected area and average ratio of wing chord/perimeter.

Wind tunnel. A Kenney Engineering Corporation model 1057 closed-circuit wind tunnel (single return) was used. The working section was 0.26 × 0.30 m. The turbulence factor for the wind tunnel was determined by measuring the drag coefficient of a sphere (0.1 m diam.) at different Re (Pope & Harper, 1966). The drag coefficient of the

sphere declined markedly at $Re = 1.6 \times 10^6$, hence the turbulence factor is quite low, at about 2.4.

Wind velocity in the tunnel was measured by using a pilot tube (United sensor PAC-12-k1) and a Barocell electric manometer (sensitivity = 10^{-6} mmHg). The static and dynamic pressure heads measured with the pitot tube were converted to air velocity as described by Pope and Harper (1966).

Lift/drag measurement. Lift and drag forces were measured by using two rectilinear strain-gauge assemblies, with their movement axes mounted at 90° . Each assembly was composed of four strain-gauges for thermal stability. The strain-gauge assemblies were mounted under the floor of the tunnel, and could be rotated through an angle of about 100° with a motorized, rotating support. The lift and drag forces were calculated trigonometrically from the measured forces and the angle of rotation, since the whole strain-gauge assembly rotated. The gauges were operated with a Beckman RS Dynograph (type 462) with type 9802 strain-gauge couplers and 416 B pre-amplifiers. The output signals were time-averaged over about 5 s using a Heath Universal Digital Instrument EU-805. The strain-gauge assembly was calibrated daily by using a 0.001 N Pesola scale. Lift and drag measurements were repeatable to ± 0.002 N.

The bird wings were mounted vertically in the tunnel because the strain-gauge assembly was located under the floor of the tunnel. This attitude did not affect the aerodynamic properties of the wing to a significant extent, but meant that the mass of the wing was acting at 90° to its normal direction relative to the wing. However, the weight of the wing is generally small compared to the aerodynamic forces and can be ignored. The wings were not mounted with the root flush against the tunnel wall (as model aeroplane wings are) because of technical difficulties. The wing root hence shed a vortex wake, and the pattern of air flow around the wing root was atypical. This might increase $C_{D, \text{in}}$, but would have little effect on minimum C_D , or C_L values. The most significant effect would be to underestimate aerofoil efficiency factor. However, the data obtained with this mounting system do not indicate any significant effects (see below). Standard wall interference factors for the wind tunnel were calculated for a close-circuit, rectangular tunnel (Pope & Harper, 1966), but no corrections were required except for the induced drag of the largest wing (red-shouldered hawk) which was adjusted for the proximity of the ground-plane.

The local angle of attack of the wing was measured at mid-span with a protractor mounted on the top of the wind tunnel. Angle of attack varies along the wing, however, because of natural twist and aerodynamically induced bending.

Lift and drag coefficients (C_L , C_D) were calculated from the resolved forces using the standard equations:

$$L = \frac{1}{2} \rho V^2 S C_L, \quad D = \frac{1}{2} \rho V^2 S C_D,$$

where ρ is the air density (1.18 kg m^{-3}), V is the wind velocity (m s^{-1}), S is the projected area (m^2), L and D are the lift and drag force (Newtons) and C_L and C_D are the dimensionless lift and drag coefficients. The term $\frac{1}{2} \rho V^2$ (the dynamic pressure head) was measured with the pitot tube and electric manometer.

Pressure distribution. The pressure distribution over the leading portion of the night-hawk wing was measured at mid-span. Small (27-gauge) hypodermic needle tips were forced through the rachis (central support of the fethers) in appropriate positions,

Table 1. *Morphometric parameters for bird wings and vulture primary feather, and morphometrics of wing cross-section at approximately mid-span*

(Thickness ratio = maximum thickness/chord; camber ratio = maximum deviation of centre of wing from line connecting leading and trailing edges; nose radius ratio = approximate radius of wing at leading edge/chord; twist is base to tip twist angle.)

	Length (m)	Projected area (m ²)	Wetted area (m ²)	AR	Thickness ratio	Camber ratio	Nose Radius ratio	Twist (degrees)
Swift	0.141	0.005	0.0104	3.9	0.054	0.054	0.012	5
Petrel	0.212	0.0116	0.024	4.1	0.048	0.065	0.011	9
Woodcock	0.171	0.0137	0.029	1.9	0.053	0.081	0.019	7
Wood duck	0.257	0.0211	0.044	3.1	0.100	0.069	0.020	11
Quail	0.145	0.0109	0.023	1.8	0.036	0.101	0.019	5
Starling	0.164	0.0088	0.035	3.0	0.036	0.112	0.032	13
Nighthawk	0.260	0.0165	0.035	4.1	0.062	0.069	0.035	5
Hawk	0.394	0.0522	0.112	3.0	0.068	0.099	0.032	10
Vulture primary	0.180	0.00410	0.0086	7.9	0.063	0.039	~0	15

with the blunt end of the needle flush with the upper (or lower) surface of the rachis. The bevelled end of the needle was pushed into thin-bore Polyethylene tubing (PE 010 × 030), which was led under the secondary feathers to the base of the wing and out of the wind tunnel to the electric manometer. The needle was bent at the rachis to allow it to lie flush under the secondary feathers. This arrangement should result in minimal aerodynamic interference with the wing. The pressure at each orifice was then measured, and the values expressed in the standard manner:

$$P = (p' - q)/p,$$

where p' is the measured static pressure head at the orifice, p is the ambient dynamic pressure head and q is the ambient static pressure head (Pope & Harper, 1966). Classic lifting-line theory was used to evaluate many of the aerodynamic properties of the bird wing, rather than lifting-surface theory. All units are S.I.

RESULTS

Morphometrics. The ranges of various morphological parameters for the wings studied are shown in Table 1. Most of the wings were approximately elliptical in planform, although the hawk wing was the most rectangular and the wood duck wing was the most tapered. The surface areas ('wetted' areas) of the wings were about 2.04–2.14 times greater than the projected areas.

Lift/Drag. The absolute values of lift and drag (in Newtons) were dependent upon wind velocity although the general form of the lift-drag polar and the maximum lift/drag ratio were independent of velocity. All lift and drag data presented here are converted to the lift and drag coefficients ($C_L = 2L/(\rho V^2 S)$; $C_D = 2D/(\rho V^2 S)$) to correct for variation in dynamic pressure head ($\frac{1}{2}\rho V^2$) and wing surface area (S). The correction for dynamic pressure resulted in values of C_L and C_D which were independent of V over the narrow range of V used in this study. The aerodynamic forces at

Table 2. *Linear and quadratic regression analyses for the aerodynamic properties of bird wings and the vulture primary feather tip, as a function of the angle at attack (α)*

a = constant (α^0); b = first order term (α^1); c = second order term (α^2). Values are $\bar{x} \pm \text{s.e.}$, with the t-value for the difference from 0 in parentheses. e_1 is calculated as $1/\pi$ AR s , where s is the slope of the C_L - C_D regression, and e_2 is calculated as $4 C_D (C_L/C_D)_{\max}^2/\pi$ AR (see text).

Species	$L = a + ba$	$C_D = a + ba + ca^2$	$C_D = a + bC_L + cC_L^2$	e_1	e_2
Swift ($n = 46$)	(a) 0.027 ± 0.025 (1.1)	0.0595 ± 0.0052 (11.4)	0.052 ± 0.004 (14.7)		
	(b) 0.099 ± 0.006 (16.7)	-0.0037 ± 0.0007 (-5.2)	0.182 ± 0.014 (-12.7)	4.2	0.56
	(c) —	0.0006 ± 0.0001 (16.6)	0.280 ± 0.024 (11.5)		
Petrel ($n = 45$)	(a) 0.027 ± 0.014 (1.9)	0.0895 ± 0.0058 (15.3)	0.085 ± 0.005 (17.5)		
	(b) 0.084 ± 0.005 (17.0)	0.0049 ± 0.0008 (6.2)	0.023 ± 0.020 (-1.2)	0.24	0.43
	(c) —	0.0010 ± 0.0001 (7.3)	0.284 ± 0.030 (9.6)		
Woodcock ($n = 80$)	(a) 0.049 ± 0.023 (2.1)	0.0950 ± 0.0061 (15.6)	0.084 ± 0.004 (20.6)		
	(b) 0.053 ± 0.003 (16.8)	0.0026 ± 0.0010 (2.5)	0.049 ± 0.023 (-2.1)	0.51	0.66
	(c) —	0.0004 ± 0.0001 (4.0)	0.369 ± 0.030 (12.2)		
Wood duck ($n = 40$)	(a) -0.061 ± 0.026 (-0.6)	0.0978 ± 0.0047 (20.9)	0.105 ± 0.004 (24.1)		
	(b) 0.061 ± 0.004 (15.0)	-0.0021 ± 0.0009 (-2.4)	0.114 ± 0.025 (-11.3)	0.65	0.55
	(c) —	0.0009 ± 0.0001 (11.0)	0.355 ± 0.041 (8.7)		
Quail ($n = 60$)	(a) 0.001 ± 0.015 (0.1)	0.0720 ± 0.0046 (15.8)	0.096 ± 0.005 (20.8)		
	(b) 0.050 ± 0.001 (35.7)	-0.0007 ± 0.0003 (-2.5)	-0.282 ± 0.025 (-11.3)	0.83	1.4
	(c) —	0.0004 ± 0.0002 (16.6)	0.482 ± 0.035 (13.7)		
Starling ($n = 90$)	(a) 0.078 ± 0.017 (4.5)	0.1437 ± 0.0044 (32.4)	0.140 ± 0.004 (35.9)		
	(b) 0.060 ± 0.003 (24.0)	0.0001 ± 0.0005 (0.3)	-0.157 ± 0.015 (-10.5)	0.46	0.57
	(c) —	0.0007 ± 0.0001 (12.9)	0.400 ± 0.025 (15.8)		
Nighthawk ($n = 134$)	(a) 0.048 ± 0.010 (5.1)	0.0622 ± 0.0020 (31.8)	0.063 ± 0.002 (33.5)		
	(b) 0.078 ± 0.002 (45.3)	-0.0043 ± 0.0006 (-7.2)	-0.101 ± 0.009 (-11.7)	0.92	1.3
	(c) —	0.0010 ± 0.0001 (16.9)	0.211 ± 0.011 (19.3)		
Hawk ($n = 90$)	(a) 0.080 ± 0.012 (6.6)	0.0944 ± 0.0028 (33.2)	0.085 ± 0.004 (22.3)		
	(b) 0.055 ± 0.002 (25.3)	0.0018 ± 0.0005 (3.7)	-0.153 ± 0.017 (-8.8)	0.40	0.45
	(c) —	0.0006 ± 0.0001 (24.7)	0.555 ± 0.022 (25.7)		
Vulture Primary ($n = 28$)	(a) 0.051 ± 0.026 (2.0)	0.0518 ± 0.0100 (5.2)	0.050 ± 0.008 (6.4)		
	(b) 0.075 ± 0.003 (24.0)	0.0002 ± 0.0001 (0.2)	0.172 ± 0.018 (-9.7)	0.57	0.87
	(c) —	0.0006 ± 0.0001 (7.4)	0.284 ± 0.024 (11.7)		

Table 3. *Profile drag coefficient, maximum lift coefficient, maximum lift/drag ratio, slope of lift curve, and $1/\pi AR_e$ for bird wings and vulture primary feather (with angle of attack at mid-chord in parentheses for data from present study)*

Species	$C_{D, \text{pro}}$	$C_{L, \text{max}}$	$(C_L/C_D)_{\text{max}}$	$dC_L/d\alpha$	$1/\pi AR_e$	Reference
Swift	0.030 (+1°)	0.80 (+8°)	17 (+5°)	0.1	0.02	Present study
Petrel	0.070 (0°)	0.88 (+13°)	4.0 (+8°)	0.08	0.32	
Woodcock	0.082 (+2°)	0.90 (+15°)	3.5 (+8°)	0.05	0.33	
Wood duck	0.096 (+1°)	0.90 (+20°)	3.8 (+8°)	0.06	0.16	
Quail	0.055 (+3°)	1.10 (+25°)	6.0 (+8°)	0.05	0.21	
Starling	0.125 (0°)	1.00 (+15°)	3.3 (+7°)	0.06	0.23	
Nighthawk	0.051 (+3°)	1.15 (+15°)	9.0 (+6°)	0.08	0.08	
Hawk	0.074 (+2°)	1.0 (+25°)	3.8 (+6°)	0.06	0.27	
Vulture primary	0.024 (0°)	1.15 (+12°)	17 (+5°)	0.08	0.07	
Thrush	0.05	0.8	—	0.03	0.36	Nachtigall & Kempf (1971)
Sparrow	0.16	1.0-1.1	—	0.05	0.28	
Duck	0.11	0.9	—	0.06	0.34	
Snipe	0.11	1.0	3	0.06	0.33	Reddig (1978)
Pigeon models	0.06-0.13	0.8-1.2	2-8	0.12-0.27	0.1-0.7	Nachtigall (1979)

high wind speeds did not bend the wing sufficiently to alter the lift or drag coefficients. However, C_L and C_D would vary markedly over wider ranges of V (see Discussion).

The C_L and C_D of the various bird wings and the vulture primary feather altered markedly at differing angles of attack (α) at mid-span; the C_D - C_L curves, C_L , C_D and C_L/C_D data are summarized in Figs. 1-3. The value of α was arbitrarily measured only at mid-span, although the local α varied along the wing span because of inherent wing twist (see Table 1) and due to aerodynamic forces deforming (including twisting) the wing.

Aerodynamic parameters for the bird wings and vulture feathers were generally similar (Figs. 1-3; Tables 2, 3) although there were many qualitative differences. The relationship between C_D and C_L was generally U-shaped except at high α when C_L levelled off or even declined. Quadratic, best-fit equations were fitted to the C_D - C_L data (excluding data at high α) since the relation is, in theory, parabolic. The curves were often quadratic rather than parabolic (i.e. parabolic but shifted from the origin since the minimum C_D was not at zero lift; Figs. 1-3, Table 2). The C_D varied with α in a parabolic fashion, and the quadratic best-fit equations are presented in Table 2. The C_L was usually linear at intermediate α and relatively constant at lower and higher α . The best-fit linear equations for C_L at intermediate α are summarized in Table 2.

The profile drag coefficient (ideally determined as the minimum drag which occurs at zero lift) was from 0.024 to 0.125 but generally did not occur at the zero lift angle. The maximum C_L values varied from about 0.7 to 1.2 at α of 15-20° (Table 3). The C_L/C_D ratio was often quite variable, reflecting the errors involved in lift and drag measurement, but C_L/C_D always increased from negative values at low α to maximal values at α of 5-8°, then declined markedly at higher α . This is the expected form of the relation, but there is no theoretical equation so best-fit curves were obtained by using 10th degree polynomial equations to indicate the approximate relationship. The maximum values for C_L/C_D ($= L/D$) varied from 3.3 to 17 for the different wings and vulture feather.

The aerofoil efficiency factor (e) was calculated in two ways. Firstly, e was calculated

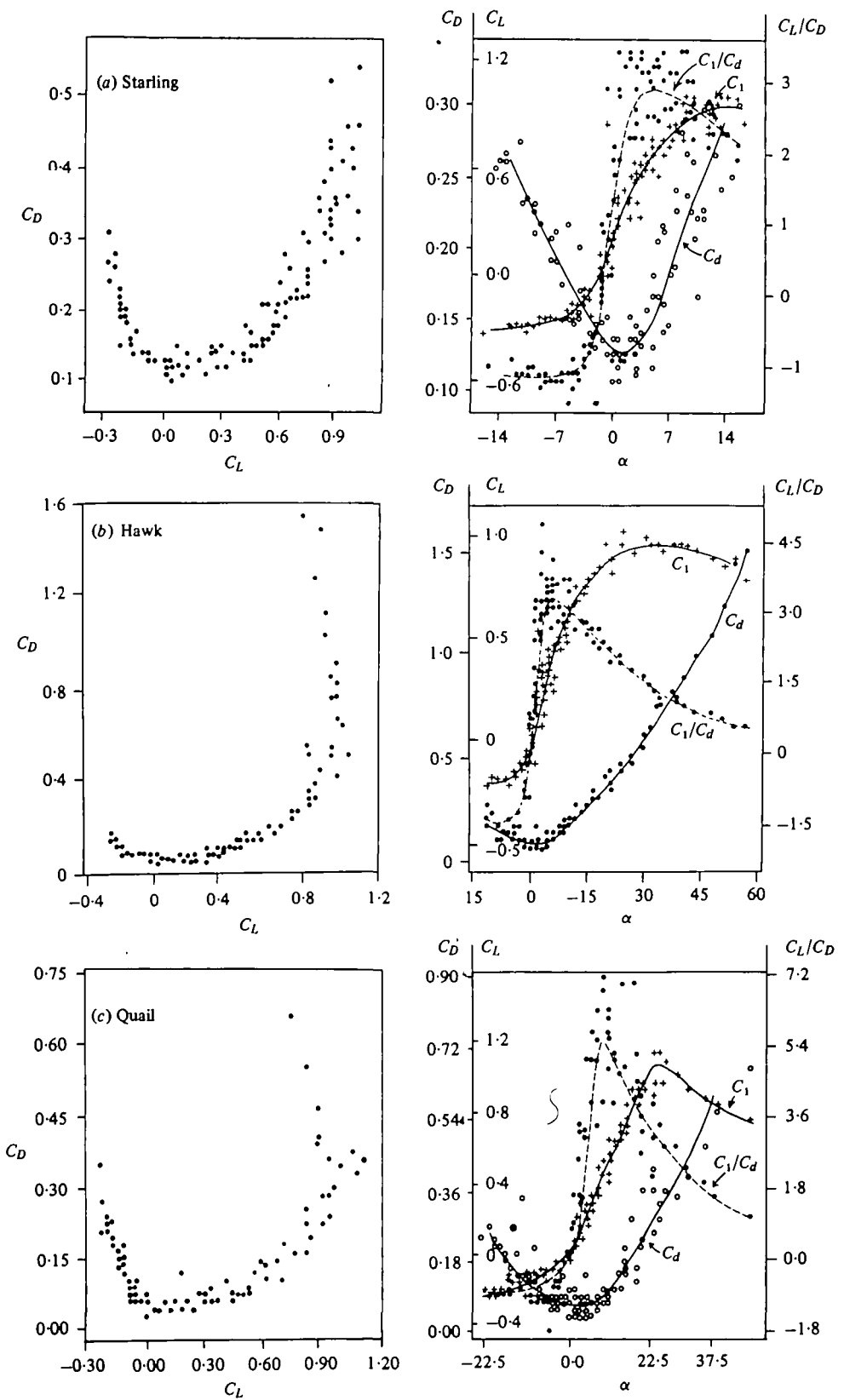


Fig. 1. For starling, hawk and quail wings. Left: lift coefficient (C_L) as a function of drag coefficient (C_D). Right: lift coefficient (C_L), drag coefficient (C_D), and lift/drag ratio (C_L/C_D) at differing angles of attack (α).

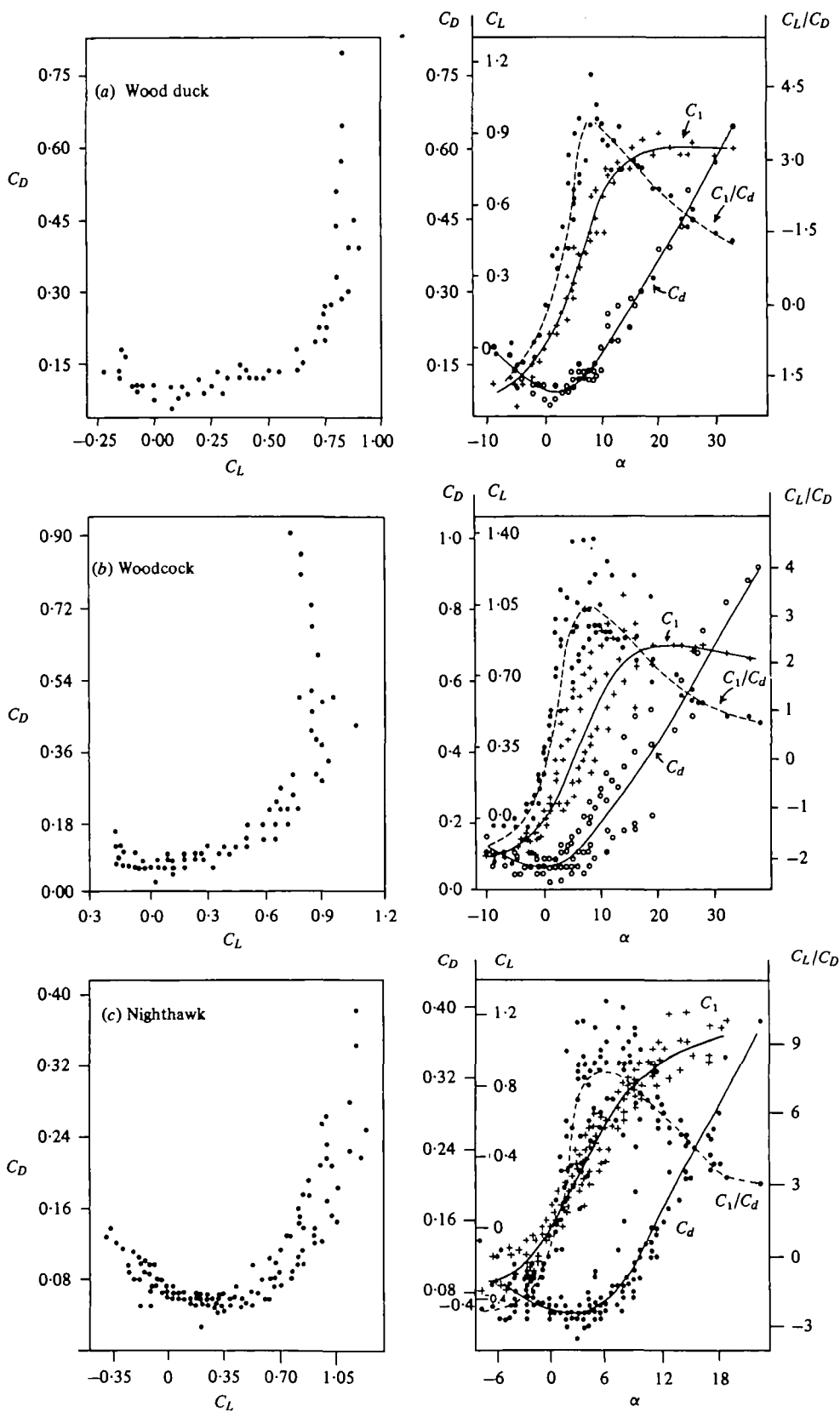


Fig. 2. For woodcock, wood duck and nighthawk wings. Left: lift coefficient (C_L) as a function of drag coefficient (C_D). Right: lift coefficient (C_L), drag coefficient (C_D), and lift/drag ratio (C_L/C_D) at differing angles of attack (α).

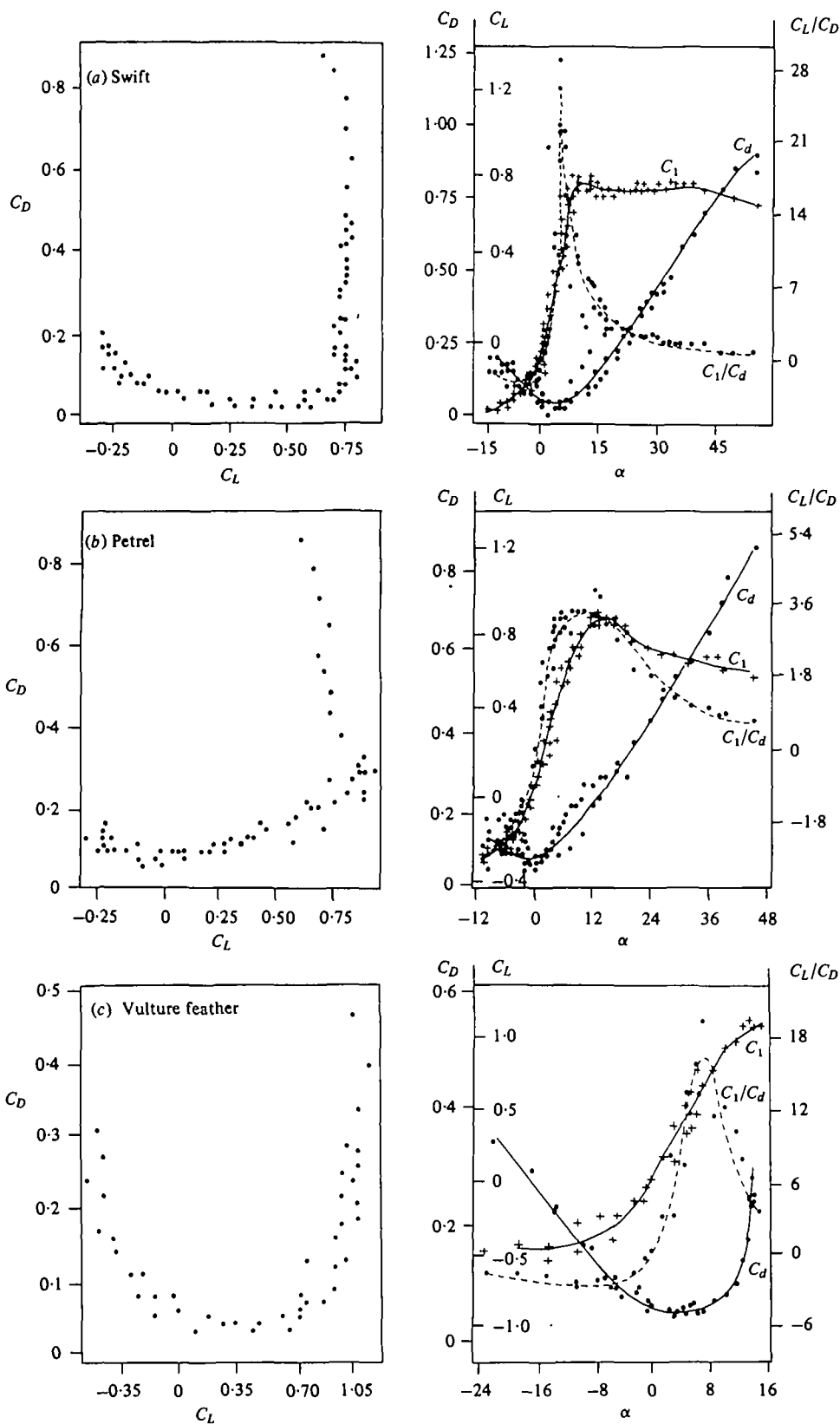


Fig. 3. For swift and petrel wings, and the tip of the vulture primary feather. Left: lift coefficient (C_L) as a function of drag coefficient (C_D). Right: lift coefficient (C_L), drag coefficient (C_D), and lift/drag ratio (C_L/C_D) at differing angles of attack (α).

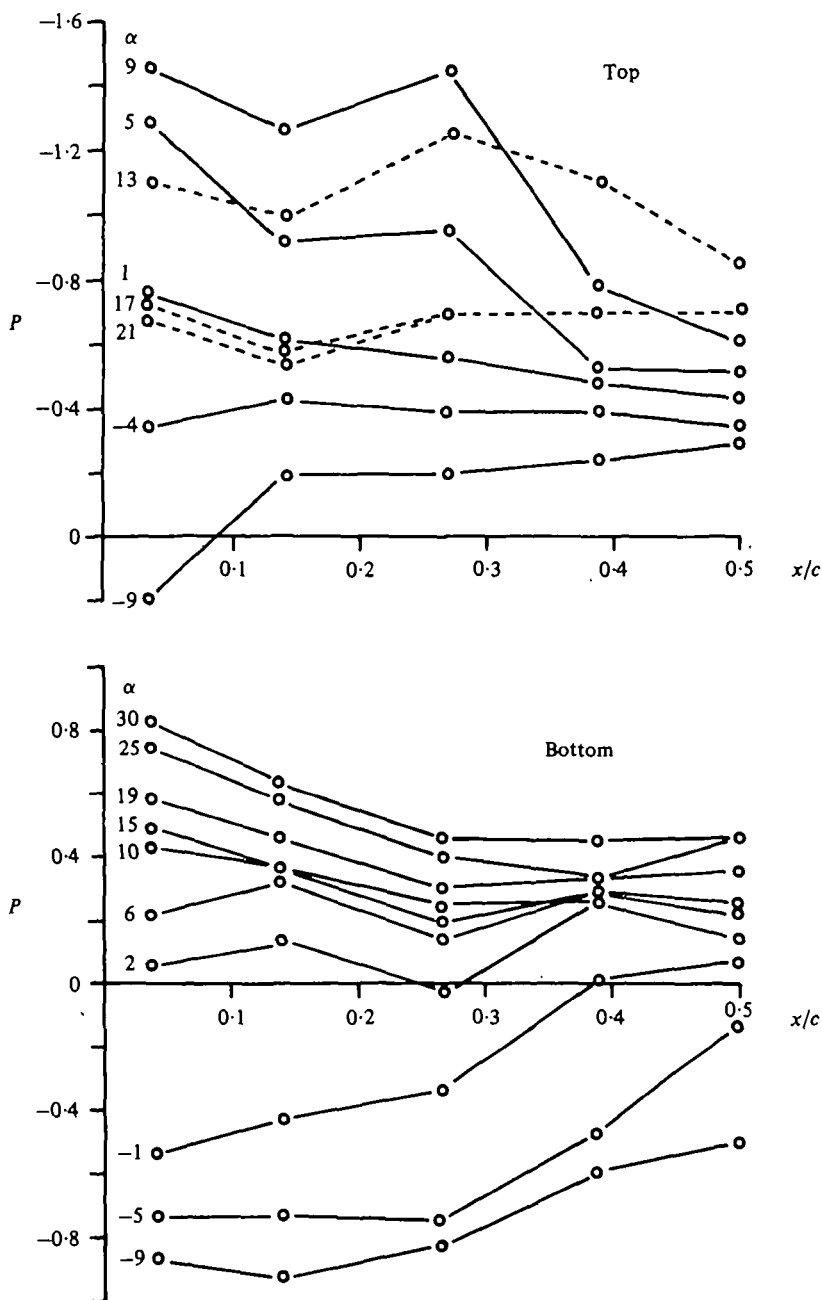


Fig. 4. Pressure distribution for the leading one half of the nightjar wing at mid-span, with differing angles of attack (α). x/c indicates position of pressure measurement relative to the wing chord (c). P is the pressure at the flush orifice corrected for ambient static and dynamic pressure heads (see text).

Table 4. Lift and pressure drag coefficients calculated for the nighthawk wing from the pressure distributions at differing angles of attack (α), compared to values measured for the wing using force transducers assuming skin friction drag coefficient was 0.02, and calculating induced drag as measured $C_L/\pi AR$ (0.9)

α	Calculated C_L	Measured C_L	Calculated $C_{D, \text{pro}}$	Measured $C_{D, \text{pro}}$
-8	-0.46	-0.40	0.06	0.08
-4	-0.13	-0.18	0.04	0.06
+2	0.44	0.29	0.03	0.04
+7	0.76	0.60	0.06	0.04
+20	0.66	1.1	0.18	0.28

from a regression of C_D and C_L since the theoretical slope of this relationship is $1/(\pi AR e)$ and the intercept is the profile drag coefficient (Greenewalt, 1975). The values of e were also calculated from the $(C_L/C_D)_{\text{max}}$ value since $e = 4C_{D, \text{pro}}(C_L/C_D)_{\text{max}}^2/(\pi AR)$ (Greenewalt, 1975). The values of e were in reasonable agreement using the two different methods, and generally ranged from 0.3 to 0.8 (ignoring the unreasonable values > 1).

Pressure distribution. The pressure distribution (expressed as P , corrected for dynamic and static pressure head) over the mid-span of the nightjar wing altered markedly at differing α (Fig. 4). The values for C_L and C_D can be calculated from these distribution data (Pope & Harper, 1966). Only the pressure for the leading one-half of the wing section was measured, but this is the most important in terms of lift and drag, so approximate calculated values for C_L and C_D are presented in Table 4. These estimated C_L and C_D values are in general agreement with C_L and C_D values measured for the whole wing.

DISCUSSION

The lift and drag characteristics of bird wings and the vulture feather resemble, in general form, those of conventional (man-made) aerofoils (e.g. Von Mises, 1959; Hoerner, 1965; Pope & Harper, 1966; Hoerner & Borst, 1975), other bird wings (Nachtigall & Kempf, 1971; Reddig, 1978; Nachtigall, 1979) and insect wings (Jensen, 1956; Vogel, 1966; Nachtigall, 1976). However, there are significant quantitative differences between the aerodynamic performances of conventional aerofoils, bird wings, and insect wings. The following discussion relates how these differences are attributable to variation in wing morphometrics and air-flow regime (i.e. Re).

Aerodynamic drag. The minimum drag coefficients measured here for the bird wings were from 0.03 to 0.13, with the primary feather tip of a black vulture having a drag coefficient of 0.024. These drag coefficients are similar to those measured for other bird wings, or parts of bird wings, or models of bird wings. Minimum drag coefficients for insect wings are similar or higher: locust forewing 0.024; locust hind wing, 0.06 (Jensen, 1956); *Drosophila* wing 0.3 (Vogel, 1966). These values for bird and insect wings are considerably higher than those for conventional aerofoils, which typically have minimum drag coefficients of less than 0.01. As will be shown below, these marked variations in minimum drag coefficient for insect, bird and man-made wings do not necessarily reflect different wing morphology or function but simply the Re at which they operate.

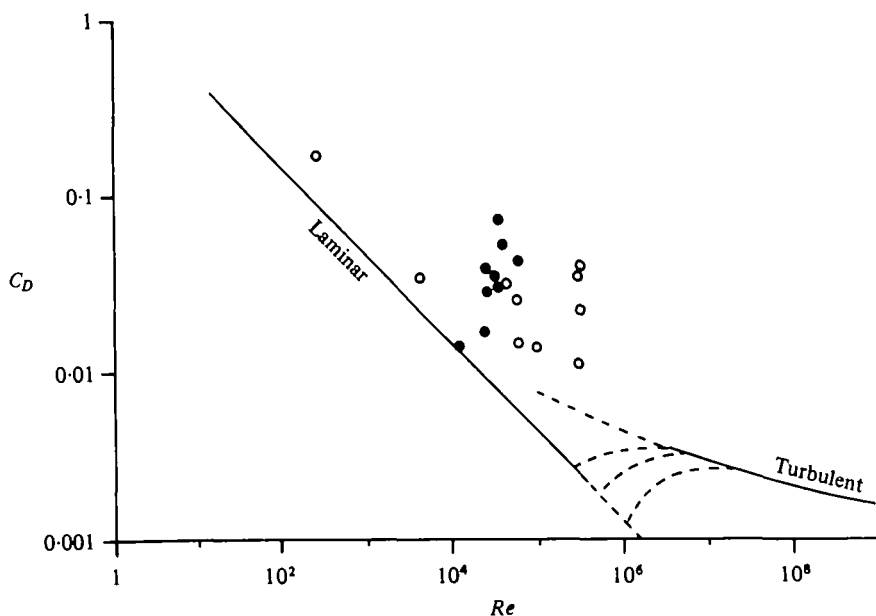


Fig. 5. Drag coefficient (C_D) for bird wings and vulture primary feather (solid circles), insect wings (open circles, below $Re = 10^4$) and other aerofoils (open circles) expressed relative to 'wetted area' (see text). Solid lines are for calculated skin friction drag coefficients, with transition from laminar to turbulent shown by broken lines. Vulture primary feather is solid circle closest to line for laminar skin friction drag coefficient. Insect wing data are from Jensen (1956) and Vogel (1966); other aerofoil data from Tucker & Parrott (1970).

There are three basic components of aerodynamic drag: skin friction drag (drag coefficient = $C_{D,f}$), pressure drag ($C_{D,pre}$) and induced drag ($C_{D,in}$). The first two drag terms are generally combined into a single term, profile drag ($C_{D,pro}$).

Skin friction depends upon the Re , and whether flow is laminar or turbulent. For laminar flow,

$$C_{D,f} = 1.33 / \sqrt{Re} \quad (\text{Blasius' equation}),$$

whereas the relationship for turbulent flow is

$$\log (Re \cdot C_{D,f}) = 0.24 / \sqrt{C_{D,f}} \quad (\text{Schoenherr's equation})$$

(see Hoerner, 1965). Transition from laminar to turbulent flow usually occurs spontaneously at Re of 10^5 – 10^6 but transition can be forced to occur at lower Re (and also occurs immediately after the thickest section of an aerofoil at low Re). Laminar $C_{D,f} \simeq$ turbulent $C_{D,f}$ in the range of Re applicable to bird wings (Fig. 5). The minimum values for C_D of bird wings are generally greater than the estimated skin friction drag coefficient, although the drag of the vulture primary feather is only slightly greater than the predicted skin friction drag (Fig. 5). (Note that the C_D values in Fig. 5 are expressed relative to 'wetted' area, rather than the projected area because it is 'wetted' area, not projected area, that determines $C_{D,f}$.) The vulture feather, not unexpectedly, had the drag coefficient most similar to its skin friction drag because it is the 'cleanest' aerodynamic shape. The C_D values of insect wings are also only a little greater than the predicted skin friction C_D (Fig. 5). Aeroplane wings, which operate at much higher Re , have correspondingly lower $C_{D,f}$ (Fig. 5).

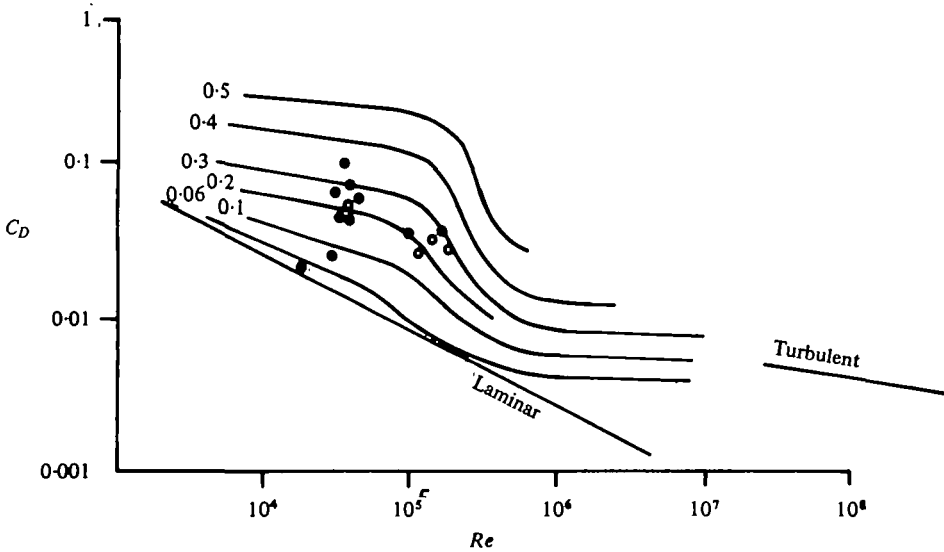


Fig. 6. Drag coefficient (C_D) for bird wings and vulture primary feather tip at differing Reynold's numbers, expressed relative to projected area, compared with values for conventional aerofoils of thickness ratios from 0.06 to 0.5, and compared to calculated skin friction drag coefficients for laminar and turbulent flow. Aerofoil data from Hoerner (1965).

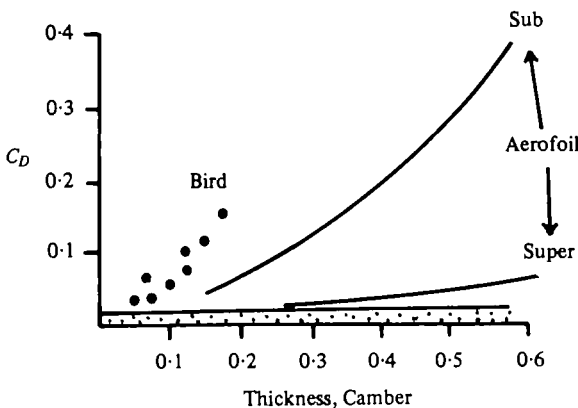


Fig. 7. Total drag coefficient (C_D) for bird wings as a function of camber, and total drag coefficients for conventional aerofoils at subcritical and supercritical Re as a function of thickness. Magnitude of skin friction drag is indicated by stippled area. Aerofoil data are from Hoerner (1965).

The pressure drag coefficient is determined by the magnitude of the turbulent wake left behind an object, and hence is lowest for streamlined bodies with delayed separation. The $C_{D, \text{pre}}$ is experimentally determined as $C_{D, \text{pro}} - C_{D, f}$. Pressure drag becomes relatively more important than skin friction to total drag at high Re since skin friction is reduced. Separation of air flow is delayed at high Re by boundary layer turbulence, and this is reflected by a dramatic decrease in $C_{D, \text{pre}}$ (or $C_{D, \text{pro}}$) at Re above a critical level, about 10^5 (Fig. 6). Conventional aerofoils, which usually operate above this critical Re , have a much lower drag than bird and insect wings. However, bird wings have higher drag coefficients (Fig. 7) than aerofoils at equivalent Re (below the critical range), perhaps reflecting the surface roughness of bird wings and the tendency of individual feathers to flutter and increase drag, or wing twist (see below).

Table 5. *Multiple linear regression analysis for aerodynamic parameters as a function of morphometric parameters, showing significantly correlated parameters (and r-values) and presenting the multiple linear regression equation (n = 9 for all analyses)*

Aerodynamic parameter	Correlated morphometric parameters	Multiple linear regression equations
$C_{D, \text{pro}}$	AR = aspect ratio ($r = -0.54$) f/c = camber ($r = 0.71$) r/c = nose radius ($r = 0.57$)	$C_{D, \text{pro}} = -0.0074 + 0.969 (f/c)$
$C_{L, \text{max}}$	x_f = position max. camber ($r = 0.67$)	$C_{L, \text{max}} = 1.24 - 0.55 (x_f)$
L/D_{max}	AR = aspect ratio ($r = 0.72$) f/c = camber ($r = 0.74$) r/c = nose radius ($r = 0.57$)	$L/D_{\text{max}} = 21.4 - 181 (f/c)$
$dC_L/d\alpha$	f/c = camber ($r = 0.70$) AR = aspect ratio ($r = 0.52$)	$dC_L/d\alpha = 0.105 - 0.48 (f/c)$
$dC_D/dC_L^{\frac{1}{2}}$	AR = aspect ratio ($r = 0.62$)	$dC_D/dC_L^{\frac{1}{2}} = 0.326 - 0.032 (AR)$

The profile drag coefficient, although markedly influenced by Re , is also dependent upon the thickness of the wing, particularly at low Re when flow separation occurs immediately after the thickest or most cambered portion of the wing. This is clearly shown by the relationship between $C_{D, \text{pro}}$ and thickness (or camber) for bird wings and aerofoils at subcritical and supercritical Re (Fig. 7). The $C_{D, \text{pro}}$ of different bird wings was correlated with aspect ratio, camber and nose-radius (Table 5). Camber would be expected to have the same effect as thickness in determining the point of flow separation, the magnitude of the turbulent wake, and the drag coefficient. Indeed, camber was the morphological parameter which best predicted $C_{D, \text{pro}}$ using multiple linear regression analysis (Table 5).

Induced drag arises from the deflection of air by a wing; $C_{D, \text{in}}$ is related to the lift coefficient and aspect ratio as:

$$C_{D, \text{in}} = C_L^2 / \pi AR.$$

Induced drag is dependent upon aspect ratio since the angle through which air must be deflected to produce a given change in momentum (hence lift) increases as aspect ratio decreases. Induced drag is also dependent upon morphological parameters such as wing planform (elliptical wings have the lowest $C_{D, \text{in}}$) and wing twist. Wing planform only slightly alters $C_{D, \text{in}}$ and can be ignored for bird wings, which tend to be elliptical in planform. Wing twist, however, can markedly increase $C_{D, \text{in}}$ by simultaneously producing positive and negative lift (which algebraically cancel out so C_L is low) but drag is high since the induced drags from positive and negative lift add together, rather than cancel. Such an effect of wing twist on $C_{D, \text{in}}$ is seen in the aerodynamic data not as induced drag, but as an apparently high profile drag coefficient. The high twist of bird wings thus contributes to their high $C_{D, \text{pro}}$ and probably explains why the minimum drag coefficients were often not observed at the angle of zero lift.

Induced drag of wings is usually greater than calculated as $C_L^2 / \pi AR$ even for elliptical, untwisted wings because a wing is not a perfectly efficient device. An aerodynamic

foil efficiency factor (e) is therefore introduced into the equation relating $C_{D, \text{in}}$ and C_L :

$$C_{D, \text{in}} = C_L^2 / \pi A R e.$$

Values for e calculated for bird wings generally were from 0.3 to 0.8, with values greater than 1 discounted as experimental error or improper calculation. For conventional aerofoils, e is typically 0.9–0.95. The interpretation of e for bird wings is somewhat different from that for aerofoils at high Re (see below).

In summary, the drag of bird wings is considerably greater than that of conventional aerofoils for a variety of reasons. Skin friction drag is higher because of the lower Re , and whether air flow over bird wings is laminar or turbulent makes little difference to the value for skin friction drag. Pressure drag is high for bird wings because the Re is subcritical and so separation occurs immediately after the thickest part of the wing; it also appears to be high because bird wings are twisted. Feathers may also result in some additional drag compared to a smooth aerofoil. Induced drag appears to be greater for bird wings, which have lower aerofoil efficiency factors. Insect wings, which operate at lower Re than bird wings, have even higher drag coefficients despite their 'cleaner' aerodynamic shapes, because of higher skin friction drag.

Aerodynamic lift. The lift coefficient for bird wings varied from about -0.4 to about $+1.2$ for the various species, depending upon the angle of attack. This is similar to the C_L values noted elsewhere for bird wings, parts of wings, or models (Table 3), and also for insect wings (Jensen, 1956; Vogel, 1966). The slope of the relationship between C_L and α (i.e. the lift curve slope, $dC_L/d\alpha$) was about 0.05–0.10 for the bird wings. Other values for bird wings are from 0.03 to 0.23 (Table 3) and data of Jensen (1956) and Vogel (1966) yield values of about 0.04 for insect wings. The lift coefficient of a thin aerofoil is, in theory,

$$C_L = 2\pi \sin \alpha,$$

where α is the angle of attack (Hoerner & Borst, 1975). The lift curve slope is calculated as:

$$dC_L/d\alpha = 2\pi^2/180 = 0.11$$

(Hoerner & Borst, 1975). However, many factors influence boundary layer adherence to a wing, and hence alter the lifting characteristics of real (and non-thin) wings. Such factors include cross-sectional shape of the wing, shape of the leading and trailing edges, thickness, camber and Re .

Lateral flow of air around wing tips is also of significance to aerofoils of low aspect ratio (< 5) such that $dC_L/d\alpha$ is higher ($= 0.5 \times AR$ up to a maximum of about 0.27; Hoerner & Borst, 1975). However, values for $dC_L/d\alpha$ of the bird wings were usually less than or equal to 0.1 (Table 2). The $dC_L/d\alpha$ for bird wings may have been underestimated slightly since the C_L - α relationship often appeared to be S-shaped (sigmoidal) but a linear regression was used to estimate the mean slope.

The maximum lift coefficient of aerofoils is predicted to be:

$$C_{L, \text{max}} = 1.04 AR / 4\pi^2$$

(Hoerner & Borst, 1975). However, actual values of $C_{L, \text{max}}$ are only 10–20% of the predicted values, even for conventional aerofoils with extensive boundary layer con-


trol. Bird wings had even lower $C_{L, \max}$ than conventional aerofoils. The $C_{L, \max}$ of aerofoils decreases at Re less than about 10^5 because the progressive increase in thickness of the boundary layer along the wing chord promotes flow separation near the leading and trailing edges (Hoerner & Borst, 1975). This propensity for boundary layer separation limits $C_{L, \max}$ to low values at $Re \leq 10^5$ for both bird wings (Figs. 1-3) and other aerofoils.

The values of $C_{L, \max}$ of bird wings measured in the wind tunnel were quite low (≤ 1.2). Similar values of $C_{L, \max}$ for bird wings are reported elsewhere (Table 3). This is in marked contrast to calculated or estimated values of $C_{L, \max}$ for birds or bird wings for gliding or flapping flight (Tucker & Parrott, 1970; Weis-Fogh, 1973; Norberg, 1975). However, Norberg (1976) calculates lower values which are more consistent with steady state for hovering bats, of about 1.4-1.6. Such high $C_{L, \max}$ values are not consistent with steady-state aerodynamics, either for the measured bird wings or conventional aerofoils at low Re . The body and tail of birds probably contribute some lift (hence C_L based only on wing projected area is overestimated). Separation of primary feathers during the wing stroke may increase the effective aerofoil area, hence use of the wing projected area would also overestimate the actual C_L (see P. C. Withers, in preparation). Further, non-steady state aerodynamics have been shown to yield higher $C_{L, \max}$ values in some instances (Weis-Fogh, 1973, 1976).

Morphological parameters, such as camber and leading-edge shape, can also affect $C_{L, \max}$. The $C_{L, \max}$ for bird wings was correlated with the position of maximum thickness, such that wings with the point of maximum thickness near the leading edge had the lowest $C_{L, \max}$. The $C_{L, \max}$ of bird wings (but not the vulture primary feather tip) was also correlated with camber ($r = 0.52$), as would be expected.

The C_L of conventional aerofoils decreases dramatically at high α , but this is not so for conventional aerofoils or bird wings at low Re . A high C_L at large α is of significance to birds during landing, when the wing may be 'stalled' at high α , with a consequently high drag to decelerate the bird, without reducing C_L . No special properties of bird wings are required to explain this lack of wing stall at high α , although Vogel (1966) suggests that insect wings are specially adapted to maintain high C_L after 'stall'.

Lift/drag ratio. The C_L of bird wings determines the angle of attack and wind velocity required for horizontal flight. The C_D determines the power required for flight (power = drag force \times velocity). The lift/drag ratio ($C_L/C_D = L/D$) reflects the performance of the aerofoil, i.e. its aerodynamic 'cleanness' and glide angle. The C_L/C_D of bird wings was maximum at small, positive α (and at low C_L values); $(C_L/C_D)_{\max}$ ranged from 3.3 for the starling wing to about 17 for the swift wing and vulture primary feather. Conventional aerofoils typically have C_L/C_D ratios of 20 or more, at high Re , but $(C_L/C_D)_{\max}$ is much lower at Re 's similar to those of the bird wings (Pope & Harper, 1966). The $(C_L/C_D)_{\max}$ of moth, butterfly and *Drosophila* wings is even lower (2-4) than that of bird wings because of their very low Re (Vogel, 1966; Nachtigall, 1976), although it is about 8-10 for locust wings (Jensen, 1955). It is clear that the $(C_L/C_D)_{\max}$, like many other aerodynamic parameters, is markedly dependent upon Re .

Aerofoil efficiency factor. The aerofoil efficiency factor, e (or Monk's span factor, )

Hoerner and Borst's factor, a' ; Tucker's correction factor, R) is a correction factor applied to the induced drag coefficient;

$$C_{D, \text{in}} = C_L^2 / \pi A R e.$$

The value of e indicates the efficiency of the wing in deflecting air in order to produce lift. The theoretical value of e is 1 for elliptical, untwisted wings, but is generally 0.9–0.95 for conventional aerofoils. The value of e is often assumed to be high for bird wings (1.0 by Pennycuik, 1969; 0.9 by Tucker, 1973) although estimates for birds are from 0.5–0.7 (Greenewalt, 1975).

It proves to be much more difficult to determine e for a bird wing than for a conventional aerofoil, and the meaning is quite different. Greenewalt (1975) states that it is possible to determine both e and $C_{D, \text{pro}}$ by plotting $C_L^2 / \pi A R$ against $C_{D, \text{total}}$ since the result is a straight line whose slope is $1/e$ and intercept is $C_{D, \text{pro}}$. However, this assumes that $C_{D, \text{pro}}$ is independent of C_L , C_D and α . In fact, the relationship between $C_L^2 / \pi A R$ and $C_{D, \text{total}}$ is clearly not linear and great care is required in selecting the range of $C_{D, \text{total}}$ used to estimate e since the slope is low (and e is high) at low α , and the slope is high (and e is low) at greater α .

Values of e calculated in this study by two different methods were generally from 0.3 to 0.8, but some values were unreasonably high. Furthermore, values of e for bird wings, are not simply an efficiency factor for the following reason. $C_{D, \text{pro}}$ is a significant portion of total drag, for bird wings, and $C_{D, \text{pro}}$ will change at differing α . Thus, $C_{D, \text{total}}$ alters by more than the change in induced drag, and includes not only the mechanical efficiency term but also the change in $C_{D, \text{pro}}$ at differing α . This is not the situation for conventional aerofoils at high Re since $C_{D, \text{pro}}$ is a less significant proportion of $C_{D, \text{total}}$ and e more closely approximates a mechanical efficiency factor ($C_{D, \text{pro}}$ also changes with α for conventional aerofoils, but it is still relatively insignificant relative to $C_{D, \text{in}}$). Values of e for insect wings range from about 0.2 (*Drosophila*) to 0.5 (*Schistocerca*) (calculated from data of Jensen, 1956; Vogel, 1966). Similarly, the value of e for a flat plate at $Re = 4 \times 10^4$ is low, at about 0.4 (calculated from data in Hoerner, 1965). It is therefore of little intrinsic value to calculate e for bird wings for this reason, except for the sake of having a value for substitution into various equations.

It is possible that the manner of mounting the wing used here (no end-plate or wall boundary as a reflecting plane) overestimated the C_D at high α . However, the values of $1/\pi A R e$ calculated for bird wings from other studies are also quite low (Table 3; $1/\pi A R e$ could not be converted to e since AR was often not given). Furthermore, Nachtigall (1979) used a double end-plate system which approximates a wing of infinite span, so induced drag should be 0 (Von Mises, 1959). Nevertheless, there was clearly a marked increase in C_D at high α , indicating that $C_{D, \text{in}}$ is a small fraction of the increase in C_D ; $C_{D, \text{pro}}$ being the most important.

Pressure distribution. The pressure distribution over the nightjar wing (Fig. 4) was similar to that over a conventional aerofoil (Harper & Pope, 1966; Hoerner & Borst, 1975), with a pronounced suction peak forming on the upper, leading edge at α of 5–9°. This suction peak diminished at lower and higher α . A positive pressure developed on the lower wing surface at moderate to high α ($\geq 2^\circ$) whereas a suction

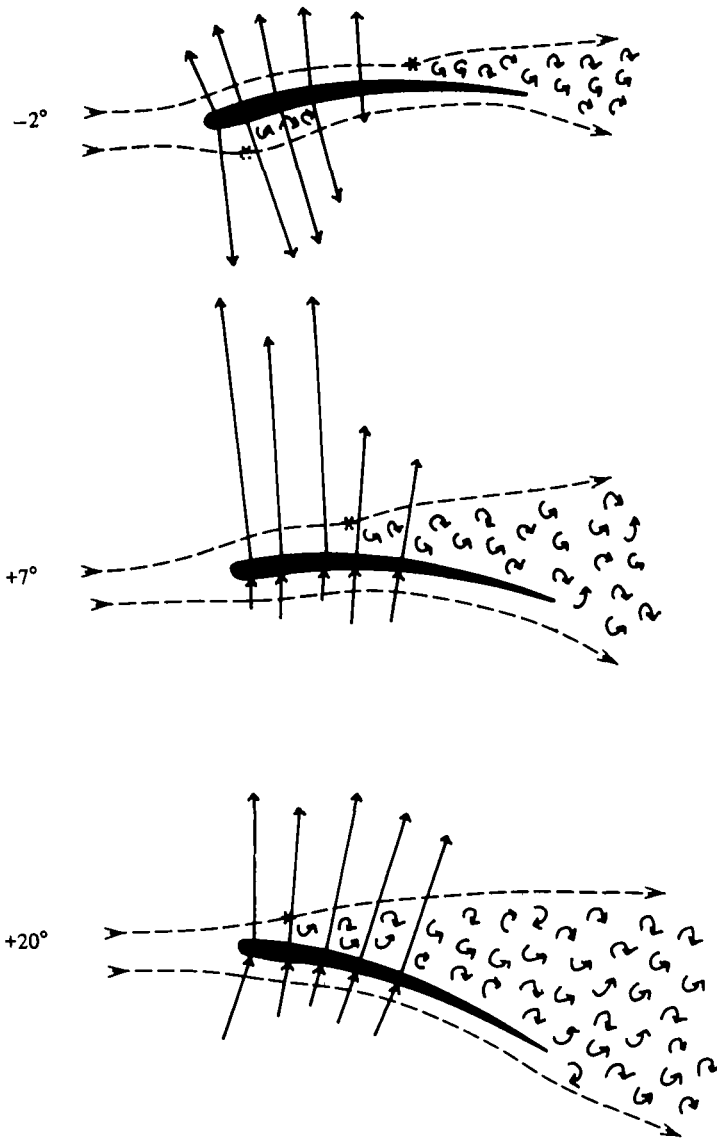


Fig. 8. Suggested pattern of air-flow over a bird wing at differing angles of attack, showing direction and magnitude of pressure distribution (solid arrows) as measured for the nighthawk wing at mid-span, the likely position of boundary layer separation (*) and regions of turbulent air flow (small arrows).

pressure formed at lower α . The relative magnitude and sign of the pressure distribution indicated the development of negative lift at $\alpha < 0^\circ$, maximum positive lift at moderate α , and a decline in lift at higher α . In fact, the actual lift and drag coefficients can be calculated from the pressure distribution (Pope & Harper, 1966). The calculations for the mid-span of the nighthawk wing, although only approximate, are consistent with the measured lift coefficients and with the pressure drag coefficient estimated from the measured C_D (the pressure distribution allows the estimation only of the pressure drag coefficient, not skin friction drag or induced drag coefficients).

The deviation of the C_L and $C_{D, \text{pre}}$ values from measured C_L and estimated $C_{D, \text{pre}}$ reflect not only potential experimental errors but also possible variation in C_L and $C_{D, \text{pre}}$ along the wing span.

The pressure distribution not only enables the estimation of local C_L and $C_{D, \text{pre}}$, but also indicates the air flow pattern over the wing. Both the pressure distribution for the nighthawk wing and basic aerodynamic considerations (Schlichting, 1966) indicate a transition from laminar to turbulent flow immediately after the thickest part of the wing, and flow separation (Figs. 4, 8). Such a flow pattern is in marked contrast to that over a conventional aerofoil, where the higher kinetic energy of the air delays turbulence and separation to a point much closer to the trailing edge than the thickest part of the wing. This difference in flow pattern for wings at low and high Re results in the higher $C_{D, \text{pre}}$ for the former. Birds, by virtue of their small wings and low flight velocity, are generally restricted to Re less than about 10^6 , although the largest flying birds may have Re 's into the transition zone and greatly benefit in terms of reduced drag and also increased lift coefficients. However, the flow pattern for a flapping bird wing may bear little resemblance to that measured in this study for a stationary wing. It would be of great interest to measure the pressure distribution or air flow of a flapping wing. Perhaps the standard boundary layer visualization techniques used for aerofoils could also be applied to bird wings.

Lift/drag relation. There is clearly an inverse correlation between the lift and drag performance of bird wings (Table 3). For example, the most streamlined wing (swift) had the lowest $C_{D, \text{pro}}$ and $C_{L, \text{max}}$, and highest $(C_L/C_D)_{\text{max}}$. The starling wing had the highest $C_{D, \text{pro}}$, a high $C_{L, \text{max}}$ and the lowest $(C_L/C_D)_{\text{max}}$. The morphology of the wings clearly contributed to these differing lift and drag performances (Table 5). The wing loading of the birds (kg m^{-2} ; from Poole, 1938, and Hartman, 1961) was not significantly correlated with $C_{D, \text{min}}$, $C_{L, \text{max}}$ or $(L/D)_{\text{max}}$, but was significantly correlated with the lift curve slope ($dC_L/d\alpha = 0.086 - 0.004$ (wing loading); $P < 0.05$). The aerodynamic performance of different bird species would seem to be determined by their wing morphology, which in turn would reflect many ecological and physiological constraints. The great variety of shape, size and aerodynamic performance of bird wings testifies to the differing trade-offs between lift and drag performance required by various bird species.

I am greatly indebted to E. Shaughnessy of the Engineering Department at Duke University for use of the wind tunnel, pitot tube and pressure sensor, and for valuable discussion. I thank P. L. O'Neill for valuable discussion. I also thank V. Tucker and K. Schmidt-Nielsen for loan of equipment.

REFERENCES

- GREENEWALT, C. H. (1975). The flight of birds. *Trans. Am. Phil. Soc.* **65**, 1-67.
 HARTMAN, F. A. (1961). Locomotor mechanisms of birds. *Smithsonian Misc. Collections*. **143** (1); 1-91.
 HOERNER, S. F. (1965). *Fluid-dynamic drag*. N.P. (Published by S. F. Hoerner.)
 HOERNER, S. F. & BORST, H. V. (1975). *Fluid-dynamic lift*. N.P. (Published by L. A. Hoerner.)
 JENSEN, M. (1956). Biology and Physics of locust flight. III. The aerodynamics of locust flight. *Phil. Trans. R. Soc. B* **239**, 511-552.
 CHITGALL, W. (1976). Wing movements and the generation of aerodynamic forces by some medium sized insects. In *Insect Flight* (ed. R. C. Rainey). *Symp. Royal Ent. Soc.* **7**, 31-46.

- NACHTIGALL, W. (1977). Zur Bedeutung der Reynoldszahl und der damit zusammenhängenden strömungsmechanischen Phänomene in der Schwimmphysiologie und Flugbiophysik. *Fortschr. Zool.* **24**, 13-56.
- NACHTIGALL, W. (1979). Der Taubenflugel in Gleitflugstellung; Geometrische Kenngrößen der Flugelprofile und Luftkraftherzeugung. *J. Ornithol.* **120**, 30-40.
- NACHTIGALL, W. & KEMPF, B. (1971). Vergleichende untersuchungen zur flugbiologischen funktion des Daumenfittichs (*Alula spuria*) bei Vögeln. I. Der Daumenfittich als Hochauftriebserzeuger. *Z. Vergl. Physiol.* **71**, 326-341.
- NORBERG, U. M. (1975). Hovering flight in the pied flycatcher (*Ficedula hypoleuca*). In *Swimming and Flying in Nature* (ed. T. Y.-T. Wu, C. J. Brokaw and C. Brennen). New York: Plenum Press.
- NORBERG, U. M. (1976). Aerodynamics, kinematics, and energetics of horizontal flapping flight in the long-eared bat *Plecotus auritus*. *J. exp. Biol.* **65**, 797-212.
- PENNYCUICK, C. J. (1969). The mechanics of bird migration. *Ibis* **111**, 178-218.
- PENNYCUICK, C. J. (1975). Mechanics of flight. In *Avian Biology* (ed. D. S. Farner, J. R. King and K. C. Parkes), pp. 1076. New York: Academic Press.
- POOLE, E. L. (1938). Weights and wing area of 143 species of North American birds. *Auk* **55**, 511-517.
- POPE, A. & HARPER, J. J. (1966). *Low Speed Wind Tunnel Testing*. New York: Wiley.
- RAYNER, J. M. V. (1979). A new approach to animal flight mechanics. *J. exp. Biol.* **80**, 17-54.
- REDDIG, E. (1978). Der Ausdrucksflug der Bekassine (*Capella gallinago gallinago*). *J. Ornithol.* **119**, 357-387.
- SCHLICHTING, H. (1966). *Boundary Layer Theory*. New York: McGraw-Hill.
- TUCKER, V. A. (1968). Respiratory exchange and evaporative water loss in the flying budgerigar. *J. exp. Biol.* **48**, 67-87.
- TUCKER, V. A. (1972). Metabolism during flight in the laughing gull, *Larus atricilla*. *Am. J. Physiol.* **34**, 841-846.
- TUCKER, V. A. (1973). Bird metabolism during flight: evaluation of a theory. *J. exp. Biol.* **58**, 689-709.
- TUCKER, V. A. & PARROTT, G. C. (1970). Aerodynamics of gliding flight in a falcon and other birds. *J. exp. Biol.* **52**, 345-367.
- VOGEL, S. (1966). Flight in *Drosophila*. III. Aerodynamic characteristics of fly wings and wing models. *J. exp. Biol.* **46**, 431-443.
- VON MISES, R. (1959). *Theory of Flight*. New York: Dover Publications.
- WEIS-FOGH, T. (1973). Quick estimates of flight fitness in hovering animals, including novel mechanisms for lift production. *J. exp. Biol.* **59**, 169-230.
- WEIS-FOGH, T. (1976). Energetics and aerodynamics of flapping flight: a synthesis. In *Insect Flight* (ed. R. C. Rainey). Blackwell Scientific Publ. *Symp. Royal Ent. Soc.* **7**, 48-72.